JOURNAL OF Materials CHEMISTRY

Theoretical approach to the design of supramolecular conjugated porphyrin polymers†

Kimihiro Susumu,[a] Hiroyuki Maruyama,[a] Hisayoshi Kobayashi[b] and Kazuyoshi Tanaka*[a]

[a]*Department of Molecular Engineering, Graduate School of Engineering, Kyoto University, Sakyo-ku, Kyoto 606-8501, Japan*
[b]*Department of Chemical Technology, College of Science and Industrial Technology, Kurashiki University of Science and the Arts, Tsurajima-cho, Kurashiki 712-8505, Japan*

Received 21st March 2001, Accepted 18th May 2001
First published as an Advance Article on the web 18th July 2001

The design of novel conjugated polymers mainly consisting of porphyrin and/or phthalocyanine rings is studied by the use of the tight-binding crystal orbital method based on the extended Hückel approximation. This paper focuses on the tuning of the electronic structures of these polymers by ethynyl bridging as well as various linkage modes. It has been clarified that the bridging sites (*meso*-to-*meso*, *meso*-to-β and β-to-β) and the bridging patterns (linear or zigzag) in the ethynyl-bridged porphyrin polymers are crucial for tuning the π-conjugation throughout the main chain. Furthermore, comparison of two-dimensional (2D) porphyrin polymer sheets and stacked porphyrin polymers demonstrates quite different electronic properties.

Introduction

The electronic properties of a one-dimensional (1D), linear π-conjugated polymer can be tuned by introducing, for instance, aromatic units, bridging units and electron-donating or -withdrawing substituents into its main chain. This class of materials has been widely investigated hitherto in relation to organic conductors,[1] nonlinear optics,[2] light-emitting diodes,[3] field-effect transistors[4] and photovoltaic devices.[5] Extension of the dimensionality of these materials by chemical or physical modifications is expected to further enhance the π-conjugation. In this context, employment of supramolecular π-systems as the unit cell is of interest for the design of chemically linked molecular sheets, self-organized polymer films and possibly novel electronic devices.

Porphyrins are tetrapyrrolic conjugated systems, the electronic properties of which can be tailored by variation of the peripheral substituents at the *meso*- or β-positions as well as of the central metals. Various multiporphyrin systems have been synthesized and investigated to determine and mimic the electron- and energy-transfer mechanisms of natural photosynthetic reaction centers and light harvesting complexes[6] and also to improve catalytic activities for the reduction of O_2.[7] Porphyrin monomer has a smaller energy gap between the highest occupied molecular orbital (HOMO) and the lowest unoccupied MO (LUMO) as compared with the other molecules that are used to construct common aromatic polymers. Moreover, the twelve peripheral sites (four *meso*- and eight β-positions) of the porphyrin ring give structural variety to porphyrin polymers. These intrinsic merits of the porphyrin thus make it a potential precursor for the construction of supramolecular π-conjugated systems. However, strategies for the modulation of the electronic properties of the porphyrin have been limited since the peripheral sites of the porphyrin are sterically crowded. In fact, phenyl or ethenyl groups attached to the *meso*- or β-positions are twisted due to steric congestion at the porphyrin peripheries, resulting in small π-overlap between the porphyrin and these "bridges".[8] On the other hand, triple bonds such as ethynyl or butadiynyl groups are cylindrically π-symmetric and, hence, are useful for keeping the adjacent porphyrins coplanar and maximizing the π-overlap among them. Recent developments in synthetic methodologies, such as metal-mediated cross-coupling, have opened up new areas of conjugated porphyrin chemistry.[9,10] Absorption spectra of these conjugated porphyrin arrays exhibited broad and well split Soret bands and intense red-shifted Q bands, features of which are more pronounced as the conjugation length increases.[9–12] Electrochemical data of the conjugated porphyrin dimers also showed reduced HOMO–LUMO gaps.[9a,13] These experimental results indicate extraordinarily enhanced π-conjugation through the triple bonds in the porphyrin arrays. Compared with many other conjugated polymers, ethynyl-bridged porphyrins make it possible to tune the absorption and fluorescence wavelengths over a wide range.

In order to develop new areas of conjugated polymeric materials, we need to thoroughly understand the electronic structures of ethynyl-bridged porphyrin polymers. In our previous report, we discussed the electronic structures of two-dimensional (2D) ethynyl- and phenyl-bridged porphyrin polymers and demonstrated that the former are promising candidates as novel electronic materials due to extensive porphyrin–porphyrin π-conjugation through their ethynyl bridges.[14]

In this paper, we report how different bridging modes affect the electronic structures of the 1D and 2D porphyrin polymers. This study aims to understand the evolution of electronic structures of a series of porphyrin polymers and the tuning of the electronic conjugation along the sequential structures of these polymers. Phthalocyanine polymers are also examined since phthalocyanine is a more extended π-aromatic system and hence has a smaller HOMO–LUMO gap than porphyrin. Zinc was utilized as the central metal of the porphyrin and phthalocyanine, since zinc porphyrins have often been used in the architecture of oligomeric porphyrins[6a,c,8] probably due to its tractability. Furthermore, the perturbation of the electronic structure was examined with respect to the stacked aggregates comprised of the 1D linear porphyrin polymers.

†Electronic supplementary information (ESI) available: Figs. A–I (see text for details). See http://www.rsc.org/suppdata/jm/b1/b102614n/

 DOI: 10.1039/b102614n

Calculation methods

The electronic structures of 1D and 2D systems of the porphyrin and phthalocyanine polymers (see Figs. 1 and 2) have been examined using the tight-binding crystal orbital (TBCO) method[15] under the extended Hückel approximation.[16]

The geometry of the planar porphyrin ring was the same as that used previously.[14] The phthalocyanine structure was taken from ref. 17. Typical bond-length data were employed for the ethynyl moieties (1.46 and 1.20 Å, respectively, for C–C and C≡C bond lengths) and the benzene ring (1.39 Å for C–C). Coplanarity between each ring in all the ethynyl-bridged porphyrin and phthalocyanine polymer model systems was assumed except for in the rotational-angle dependence calculations.

The atomic parameters employed here were taken from ref. 18. Extended Hückel calculations for organometallic compounds tend to cause unexpectedly large negative gross atomic populations. To minimize this tendency, possibly down to a level commensurate with that found in Hartree–Fock (HF) calculations, we adopted the so-called Wolfsberg–Helmholz

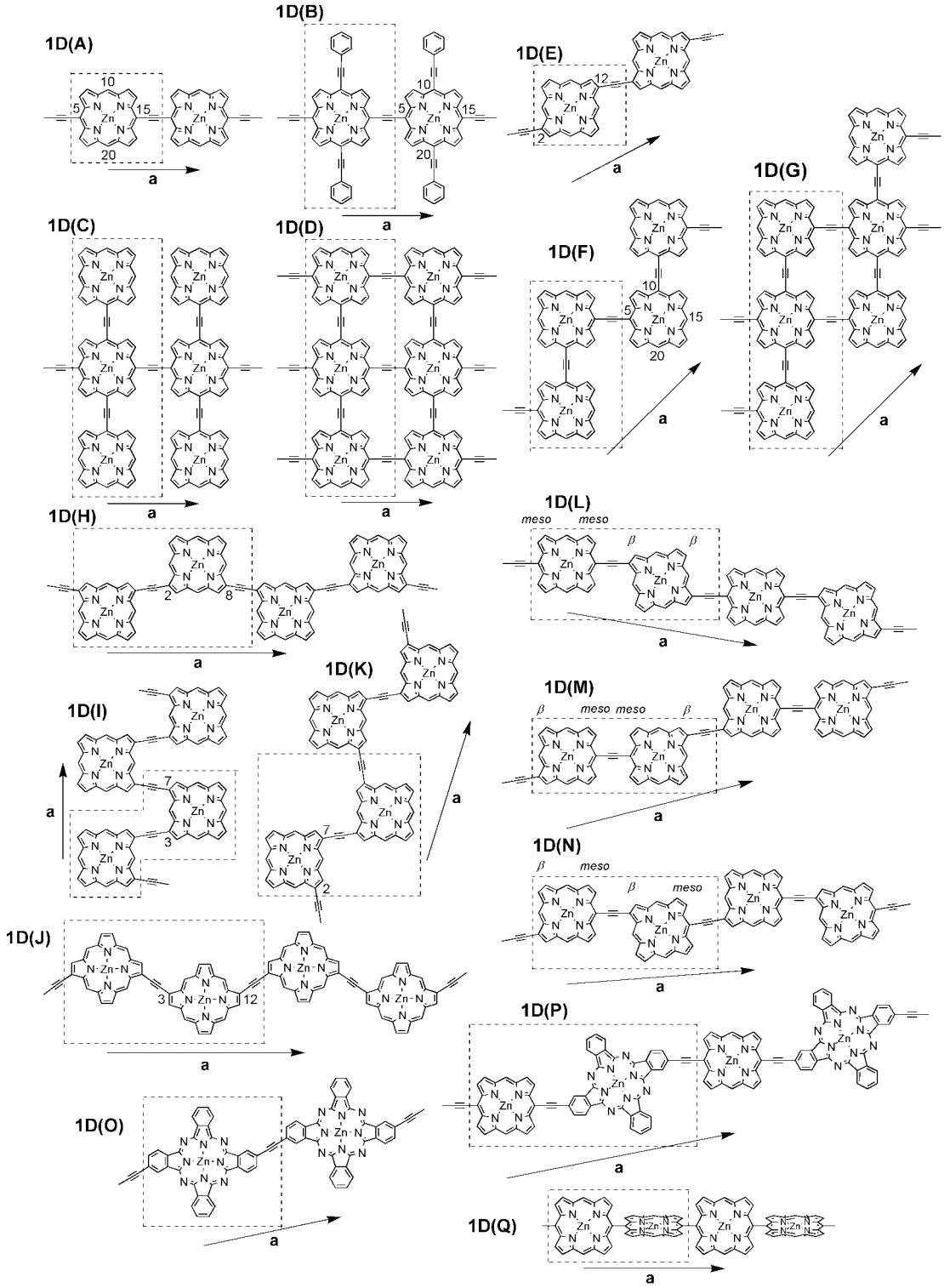

Fig. 1 Structures of the 1D porphyrin and phthalocyanine polymers examined here with the translational axis *a*. Each unit cell is enclosed by dashed lines.

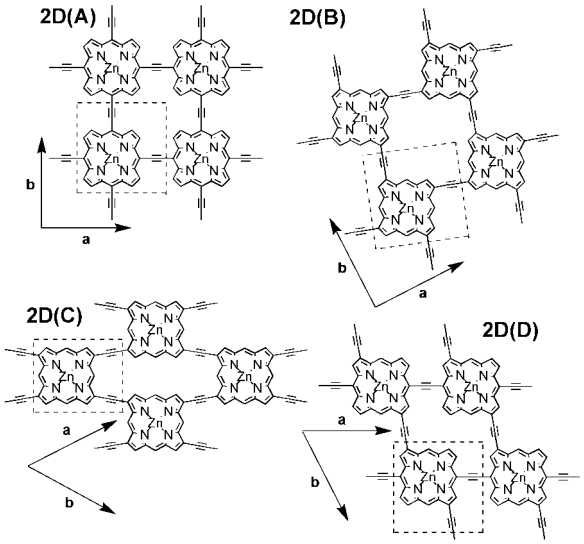

Fig. 2 Structures of the 2D ethynyl-bridged porphyrin polymers examined here with the translational axes *a* and *b*. Each unit cell is enclosed by dashed lines.

formula for the off-diagonal matrix elements H_{ij} as defined in eqns. (1)–(3) with the usual notation.[19] A considerable improvement was reported for ferrocene through the use of this correction.[19]

$$H_{ij}=\tfrac{1}{2}KS_{ij}(H_{ii}+H_{jj}) \quad (1)$$

$$K=k+\Delta^2+\Delta^4(1-k);\ k=1.75 \quad (2)$$

$$\Delta=(H_{ii}-H_{jj})/(H_{ii}+H_{jj}) \quad (3)$$

Band structures were calculated on the selected lines in the first Brillouin zone. The number of representative wave vectors (k) was chosen as 11 with regular intervals on the Γ–X line for the 1D systems and on the Γ–X, Γ–Y, X–L, and L–Γ lines for the 2D systems, respectively. For all the polymers, the overlap integrals were considered up to the nearest neighboring cell interaction since the translational length is long enough for the present calculations.

In order to evaluate the reliability of the extended Hückel method in this study, we have examined the experimental HOMO–LUMO gaps of *meso*-diethynylporphyrin monomers, ethynyl- and butadiynyl-bridged porphyrin dimers, and ethynyl- and butadiynyl-bridged porphyrin trimers, and also calculated the HOMO–LUMO gaps of the corresponding model compounds by the extended Hückel method (Table 1). Hückel type calculations are known to underestimate band gaps but the calculated band gaps are rather close to the experimental ones. On the other hand, it is well-known that HF level calculations greatly overestimate the band gaps of conjugated polymers.[20] Furthermore, the higher-level *ab initio* methods may not be suitable for an infinite chain with large aromatic molecules such as porphyrins because of the computational cost. Although the extended Hückel method is rather simple and modest in terms of the calculation level, the electronic structures of organic polymers containing transition metals have been reported with qualitative rationality.[21–26] Also, this method can be well-parametrized to yield reasonable band gaps in comparison to experimental values.[20]

Anderson *et al.* extrapolated the band gap of a butadiynyl-bridged porphyrin polymer from available optical band gaps of butadiynyl-bridged porphyirn oligomers. Their plot of optical band gap against reciprocal chain length gives a predicted band gap for the polymer of 1.55 eV from absorption and 1.34 eV from emission.[10b] A similar plot for ethynyl-bridged porphyrin oligomers[9] also predicts a band gap for the polymer of ~1.3 eV. Considering the rotational diversity around the cylindrical triple bonds of the polymer, the predicted band gap must be smaller in the ideal coplanar polymer. These experimental data also indicate that our calculated band gap of *meso*-to-*meso* ethynyl-bridged porphyrin polymer 1D(A) (1.15 eV) would be close to the experimental values. For these reasons, the present method we employed is useful in predicting the electronic properties of our systems.

Table 1 Calculated and experimental HOMO–LUMO gaps (eV) of porphyrin monomers, dimers and trimers with triple bonds. For the structure of porphyrins in this table, see the electronic supplementary information (ESI), Fig. A

		Experimental			
		Ref. 9		Ref. 10	
	Extended Hückel	Abs[a]	Em[a]	Abs[a]	Em[a]
Diethynyl monomer	1.48	1.96[b]	1.94[c]	1.92[e]	1.91[e]
Dimer	1.38	1.81[b]	1.72[b]	1.67[e]	1.66[e]
Trimer	1.32	1.55[d]	1.48[d]	1.62[e]	1.53[e]

[a]All the experimental values were converted from the lowest absorption maxima and the highest emission maxima. [b]In $CHCl_3$. [c]In THF. [d]In $CHCl_3$–pyridine (10 : 1). [e]In CH_2Cl_2–pyridine (1%).

Results and discussion

1D porphyrin polymers

In order to evaluate the degree of conjugation between the porphyrin rings in simple systems, we first examined the electronic structures of the 1D polymers consisting of the ethynyl porphyrins [1D(A)–1D(N)] shown in Fig. 1. The band structure of *meso*-to-*meso* ethynyl-bridged linear porphyrin polymer 1D(A) is shown in Fig. 3. As the wave vector k increases, the HO (π_b) band becomes stabilized and the LU (π_c) destabilized, whereas the π_a and π_d bands remain rather flat. The electronic structures of porphyrin molecules have been well explained by Gouterman's four-orbital model,[27] which is also useful for understanding the evolution of the band structures of our porphyrin polymers. This model describes the low-lying $\pi\rightarrow\pi^*$ excited states of porphyrins in terms of the transition between nearly degenerate HOMOs, $a_{1u}(\pi)$ and $a_{2u}(\pi)$, to

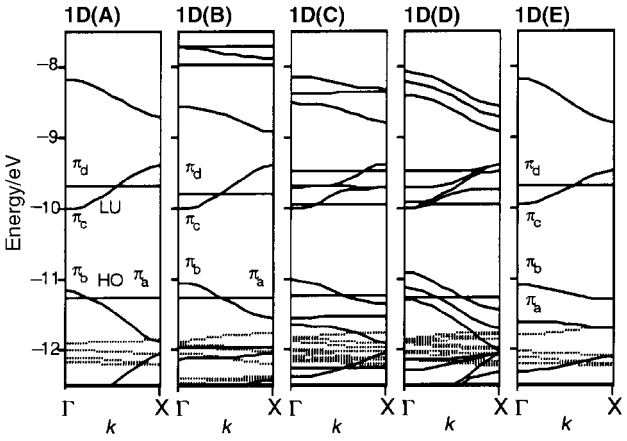

Fig. 3 Band structures of the 1D *meso*-to-*meso* ethynyl-bridged linear porphyrin polymers [1D(A)–1D(D)] and β-to-β analogue [1D(E)]. The labels Γ and X designate $k=0$ and π/a, respectively, where a is the unit length of the a axis. Solid lines indicate π-type bands and dotted lines σ-type ones, and HO and LU denote the highest occupied and the lowest unoccupied bands, respectively, throughout this article. The labels (π_a–π_d) are used to help explain the band evolution.

doubly degenerate LUMOs, $e_g(\pi^*)$ (see Fig. 4). The a_{1u} orbital has nodes at all the pyrrole nitrogens and *meso*-positions and, therefore, would remain relatively unaffected by the change of central metal and *meso*-substituents. On the other hand, the a_{2u} orbital has large coefficients at these positions. The HO- and the (HO−1)COs mostly consist of these orbitals and are closely related to the electronic properties of the porphyrin polymers discussed here as a whole.

For 1D(A) the CO pattern of the π_b band at the Γ point originates from the a_{2u} MO where the ethynyl group is attached to the *meso*-position in an antibonding manner as shown in Fig. 5. The ethynyl group is attached to the *meso*-position in a bonding manner in the π_b CO at the X point. The π_a CO originates from the a_{1u} MO and its nodes at the *meso*-positions cut off the electronic interaction between the unit cells, probably resulting in a flat band. The LU- and the (LU+1)COs originate from two degenerate e_g MOs (say, e_{gx} and e_{gy}) of the porphyrin. In the π_c CO the 5,15-*meso*-carbons along the translational axis have large coefficients and are electronically connected to the ethynyl bridges. These *meso*-carbons are attached to the ethynyl bridges in a bonding and antibonding manner at the Γ and X points, respectively. In the π_d CO this interaction is interrupted, as in the π_a CO. Thus, the a_{2u}- and e_{gx}-derived COs contribute to the extension of the π-conjugation through the ethynyl bridges and dominate the electronic structures of the *meso*-to-*meso* linkage mode.

Substitution of two phenylethynyl groups at the 10,20-*meso*-positions in 1D(B) destabilizes the π_b band and stabilizes π_d in accordance with the antibonding and bonding characteristics of the attached phenylethynyl groups, respectively (see ESI, Fig. B). On the other hand, the π_a and π_c COs are not affected by these groups. Substitution of two porphyrinylethynyl groups at the 10,20-*meso*-positions in 1D(C) shows similar shifts of these bands, although three times as many bands appear near the frontier level (some flat bands are entangled) as shown in Fig. 3. Nearly identical energy levels of the three porphyrin rings in the unit cell cause more appreciable orbital interactions than in 1D(B), resulting in larger band shifts. Substitution of the porphyrinylethynyl groups decreases the ionization potential, whereas the electron affinity is unchanged as listed in Table 2. A further decrease of the ionization potential results in a reduced bandgap for 1D(C). In the laddered polymer 1D(D), the two peripheral porphyrin rings are also connected by ethynyl bridges between unit cells, which induces further change in its band structure (Fig. 3); that is, destabilization of the HOCO results in reduced bandgap,

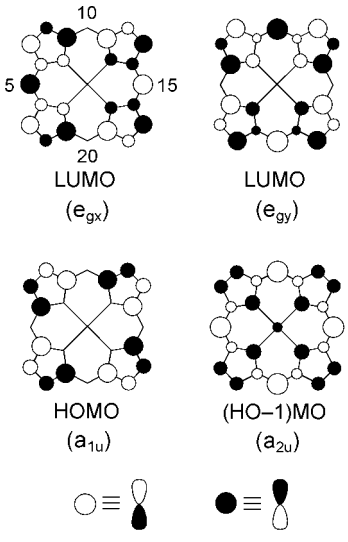

Fig. 4 Frontier MO patterns of a Zn porphyrin molecule. Note that all the AO lobes are of π-type and that the size of the circle is proportional to the magnitude of the LCAO coefficient throughout this article.

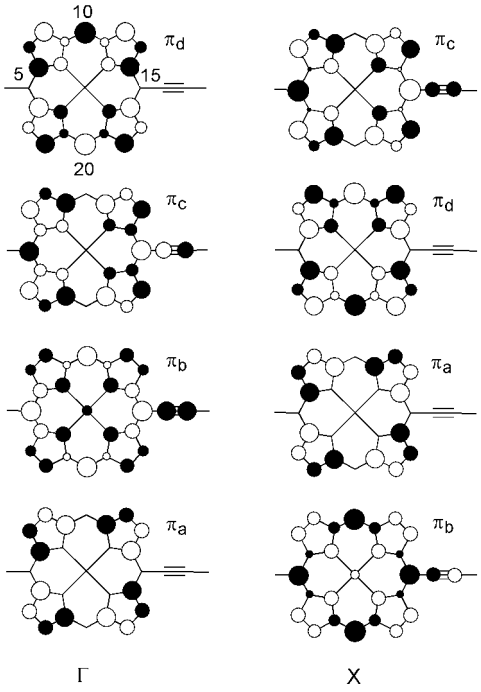

Fig. 5 Frontier CO patterns of 1D(A) at the Γ and X points.

indicating that extension of the π-systems in the unit cell, as well as multiple conjugative bridges between the unit cells, are crucial for making small bandgap polymers, as would be expected.

A porphyrin ring has four *meso*-positions and eight β-positions at its periphery. Different combinations of these positions can be utilized for substitution, making it possible to construct 1D or 2D porphyrin polymers with various linkage topologies. In 2,12-β-to-β linear porphyrin polymer 1D(E) (Fig. 3) the HO- and the (HO−1)CO patterns are derived from the a_{1u} and a_{2u} MOs, respectively (see ESI, Fig. C), whose bandgap (1.14 eV) is almost the same as that of 1D(A) (1.15 eV). However, comparison of the bandwidths with those of 1D(A) (Table 2) indicates that the π-conjugation is less effective in the β-to-β linear porphyrin polymer 1D(E).

Variation of the bridging sites in 5,10-*meso*-to-*meso* zigzag porphyrin polymer 1D(F) causes doubling of the unit cell within the framework of the computation program employed here and hence sticking of the bands as shown in Fig. 6. Both the π_a and π_d COs at the Γ point originate from the a_{2u} MO of porphyrin (see ESI, Fig. D), whereas the π_b and π_c COs from the a_{1u} MO and the accompanying bands are completely degenerate and flat. In fact, the latter COs do not contribute to extension of the π-conjugation through the adjacent porphyrin rings. Two pairs of the unoccupied COs [LU- and (LU+1)COs, (LU+2) and (LU+3)COs] are accompanied by practically flat bands.

Such characteristics of the band structures in the zigzag polymer can be explained by the frontier orbital patterns: The a_{2u}-derived π_a and π_d COs have large coefficients at all the *meso*-carbons with the bonding or antibonding interaction with the ethynyl bridges. The a_{1u}-derived π_b and π_c COs are rather isolated in each porphyrin ring. These orbital patterns result in essentially similar band structures of the occupied COs near the frontier level in both the linear and the zigzag polymers. Since both the 5- and 10-positions originally do not have the e_g MO lobes (see Fig. 4), the linkage mode in 1D(F) is not effective for π-conjugation, which results in practically flat LU bands as seen in Fig. 6. Suppression of electronic delocalization of the LU- and the (LU+1)CO decreases the electron affinity in 1D(F) (9.89 eV), increasing the bandgap (1.28 eV). Another type of *meso*-to-*meso* ethynyl-bridged zigzag porphyrin polymer,

Table 2 The calculated electronic properties (eV) of the 1D porphyrin and phthalocyanine polymers with various linkage modes

	Ionization potential	Electron affinity	HO bandwidth	LU bandwidth	Bandgap
Zn porphine	11.25	9.71			1.54[a]
Zn phthalocyanine	10.68	9.91			0.77[a]
1D(A)	11.16	10.01	0.73	0.63	1.15
1D(B)	11.04	10.01	0.50	0.63	1.03
1D(C)	11.00	10.01	0.36	0.29	0.99
1D(D)	10.91	10.01	0.53	0.53	0.90
1D(E)	11.09	9.95	0.22	0.48	1.14
1D(F)	11.17	9.89	0.72[b]	0.04[b]	1.28
1D(G)	11.01	9.95	0.32	0.04	1.06
1D(H)	11.13	9.91	0.18[b]	0.17[b]	1.22
1D(I)	11.10	9.94	0.21[b]	0.21[b]	1.16
1D(J)	11.11	9.92	0.20[b]	0.18[b]	1.19
1D(K)	11.10	9.85	0.21[b]	0.03[b]	1.25
1D(L)	11.11	9.98	0.10	0.22	1.13
1D(M)	11.16	9.97	0.02	0.18	1.19
1D(N)	11.18	9.97	0.04[b]	0.26[b]	1.21
1D(O)	10.63	10.02	0.09	0.20	0.61
1D(P)	10.66	10.02	0.02	0.11	0.64
1D(Q)	11.14	9.79	0.22[b]	0.20[b]	1.35

[a]Data for $E_{LU}-E_{HO}$, where E is the MO energy. [b]For the π bands that stick together at the X point, the bandwidth is defined by regarding these two π bands as one.

1D(G), shows a band structure similar to that of 1D(F), although the degeneracy at the X point is removed (Fig. 6). The bandgap of 1D(G) decreases (1.06 eV) due to a slightly more extended π-system than 1D(F).

The band structures of four different types of β-to-β ethynyl-bridged zigzag porphyrin polymers 1D(H)–1D(K) (Fig. 7) again show the band sticking at the X point due to the screw axis symmetry. The 2,8-, 3,7-, and 3,12-β-to-β zigzag porphyrin polymers [1D(H), 1D(I) and 1D(J), respectively] show essentially similar band structures, and their electronic properties (Table 2) resemble those of linear 1D(E) except for the LU bandwidths. On the other hand, the band structure of 2,7-β-to-β ethynyl-bridged zigzag porphyrin polymer 1D(K) shows almost degenerate LU and (LU+1) bands rather similar to those of the 5,10-*meso*-to-*meso* polymer 1D(F). Hence, the conduction band of 2,7-β-to-β zigzag polymer 1D(K) is slightly different from those of other three β-to-β zigzag polymers 1D(H)–1D(J).

The 1D *meso*-to-β linear porphyrin polymers [1D(L), 1D(M) and 1D(N)] also have screw-axis symmetry and show very narrow HO and (HO−1) bands (Fig. 8). The bandwidths of the LU- and the (LU+1)COs depend on the combination of various bridging sites of the porphyrin rings: The bandwidths of the above linear polymers are larger than those of the corresponding zigzag polymers (data not shown here). This tendency is also seen in the *meso*-to-*meso* and β-to-β porphyrin polymers. The bandgap values of these *meso*-to-β and β-to-β porphyrin polymers are almost the same, suggesting that the linking of the *meso*- and β-positions through the ethynyl bridge sites does not appreciably enhance π-conjugation.

From the above examination of the 1D ethynyl-bridged polymers, the relative magnitude of π-conjugation decreases in the order of *meso*-to-*meso* > *meso*-to-β ≈ β-to-β. This tendency

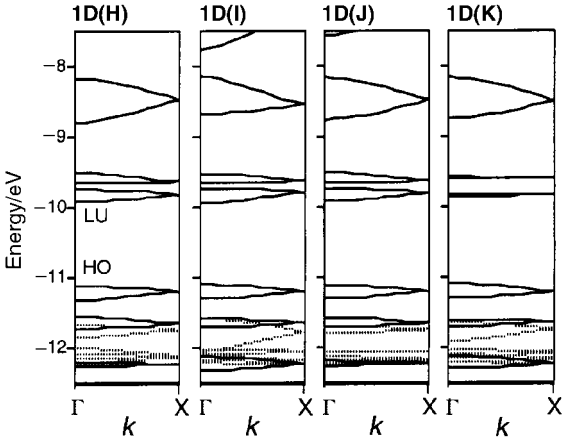

Fig. 7 Band structures of the 1D β-to-β ethynyl-bridged zigzag porphyrin polymers [1D(H)–1D(K)].

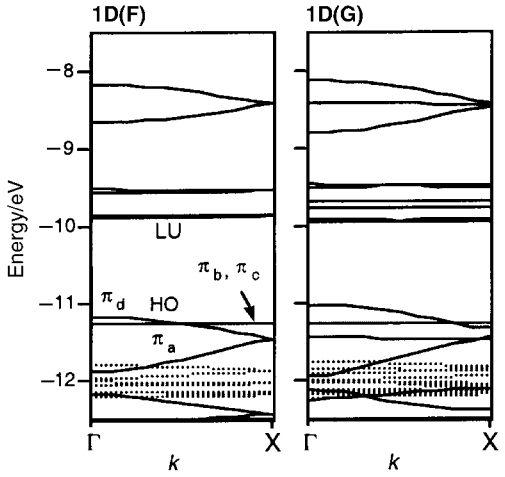

Fig. 6 Band structures of the 1D *meso*-to-*meso* ethynyl-bridged zigzag porphyrin polymers [1D(F) and 1D(G)].

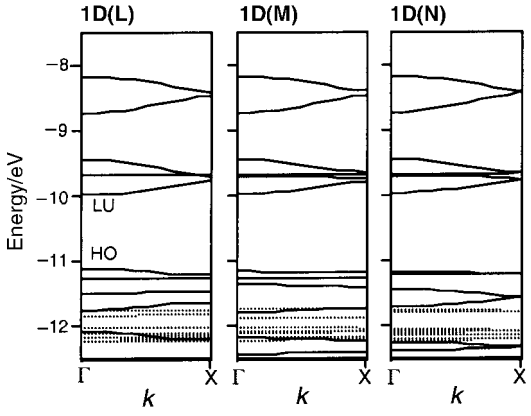

Fig. 8 Band structures of the 1D *meso*-to-β ethynyl-bridged linear porphyrin polymers [1D(L)–1D(N)].

is in agreement with the experimental results found for ethynyl-bridged porphyrin dimers (*meso*-to-*meso*, *meso*-to-β and β-to-β) by Therien and Lin,[9b] who also explored the role of porphyrin-to-porphyrin linkage topology to control the photophysical properties (although these dimer systems have different rotational angles around the ethynyl bridges).

Phthalocyanine is another attractive molecule for constructing π-conjugated polymers[28] because (i) the π-system in the unit cell is more extended than for porphyrins and (ii) its HOMO–LUMO gap is smaller than that of porphyrin. However, the band structure of ethynyl-bridged linear phthalocyanine polymer 1D(O) (Fig. 9) gives narrower HO and LU bandwidths (0.09 and 0.20 eV, respectively) than the *meso*-to-*meso* and β-to-β linked porphyrin polymers, although the bandgap is smaller (0.61 eV) probably due to underestimation of the HOMO–LUMO gap of the phthalocyanine monomer itself. The narrower HO and LU bandwidths are considered to come from (i) the separation of the π-conjugation in the HOCO at the aza nitrogens and in the LUCO at the α-carbons and (ii) the relatively small coefficients on the fused benzene rings of phthalocyanine (see ESI, Fig. E). These results are in contrast to the 1D stacked polymers composed of either porphyrins or phthalocyanines,[22] which afford no such significant difference in their band structures.

The band structure of the linear porphyrin–phthalocyanine mixed polymer alternately linked with ethynyl bridges 1D(P) is also shown in Fig. 9. The HO and LU bandwidths are smaller (0.02 and 0.11 eV, respectively) than those of the linear phthalocyanine polymer 1D(O). The CO patterns show that the two types of rings are not effectively coupled (see ESI, Fig. F), essentially due to the inherently different energy levels of the frontier MOs of the porphyrin and phthalocyanine monomers, resulting in practically flat HO and LU bands.

For the 1D porphyrin polymers discussed above, the present studies have been based on the assumption that the porphyrin rings are kept coplanar along the polymer chain. However, both experimental and theoretical investigations have suggested that structures of ethynyl-bridged porphyrin oligomers in solution have rotational diversities around the ethynyl bridges due to rather small rotational barriers.[9b,10a,29,30] In order to reveal rotational-angle dependence of the π-conjugation through the ethynyl bridge, the band structures of the *meso*-to-*meso* linear porphyrin polymer 1D(A) were checked for different rotational angles.[31] As the rotational angle is increased, the bandgap increases and the HO and LU bandwidths narrow (see ESI, Fig. G). This result simply suggests that a coplanar geometry of the polymer chain is required in order to maximize π-conjugation. Anderson and co-workers have demonstrated that formation of ladder-type complexes with bidentate ligands increases the coplanarity between the porphyrin rings in the polymer chains.[10a,d,32] Such a self-assembling method based on coordination chemistry could possibly be utilized to construct supramolecular porphyrin polymers with extensive π-conjugation. On the other hand, the band structure of the *meso*-to-*meso* directly linked linear polymer with an orthogonal geometry, 1D(Q),[33] shows somewhat dispersed frontier π bands (Fig. 10), in contrast to those of the *meso*-to-*meso* ethynyl-bridged porphyrin polymer with orthogonal geometry, which shows rather flat frontier π bands. An increase in the HO bandwidth of 1D(Q) is due to overlap of the π clouds of the a_{1u}-derived COs near the bridging sites (see ESI, Fig. H). Similar interactions of the e_{gy}-derived COs increase the LU bandwidth. Synthesized *meso*-to-*meso* directly linked porphyrin oligomers show weak red-shifts of the lowest Q bands as the number of porphyrin rings increases, suggesting that through-space π–π interaction would not be overpowering in the electronic structures of these oligomeric systems.[33] However, this result is still of interest when compared with the orbital interaction in the *meso*-to-*meso* ethynyl-bridged porphyrin polymer, 1D(A), in which the a_{2u}-derived and e_{gx}-derived COs contribute to extension of the π-conjugation. The *meso*-to-*meso* directly linked porphyrin polymer would thus offer a novel approach to construct a porphyrin polymer with unique through-space π–π interaction.

2D porphyrin polymer sheets

π-Conjugated polymers with 2D skeletons have scarcely attracted attention, with the exception of graphite, because of their difficult syntheses and intractability. However, recent efforts to synthesize board-type ladder polymers[34] as well as the proposition and synthetic challenge of novel carbon networks such as graphyne and graphdiyne[35] have highlighted 2D π-conjugated polymer sheets. As we mentioned above, porphyrin has twelve peripheral sites, and the combination of different peripheral sites for the bridges will make it possible to construct various types of 2D polymer sheets. Construction of 2D networks locks the rotation around the ethynyl bridges and hence can enhance the π-conjugation between the porphyrin rings.

The structures of the 2D porphyrin polymer sheets studied here are illustrated in Fig. 2. The aforementioned explanation for the band structures of the 1D polymers can sometimes be applied to 2D polymers. For instance, the band structure along the Γ–X line of *meso*-to-*meso* porphyrin polymer 2D(A) shown in Fig. 11 reflects that of the 1D *meso*-to-*meso* polymer 1D(A). The frontier π_b and π_d bands of 1D(A) are destabilized and stabilized, respectively, in 2D(A). The π_c and π_d bands become degenerate at the Γ and L points of 2D(A) because of the four-fold symmetry (D_{4h}) of the unit cell. Extension of the dimension

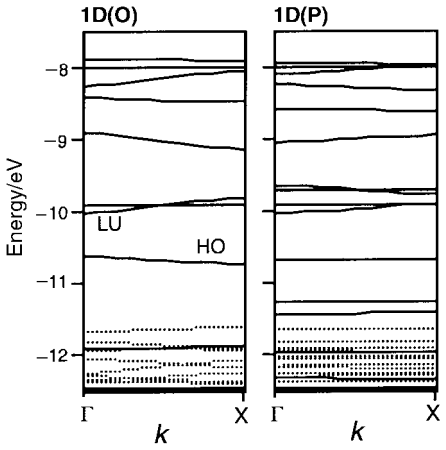

Fig. 9 Band structures of the 1D phthalocyanine polymer 1D(O) and the 1D porphyrin–phthalocyanine mixed polymer 1D(P).

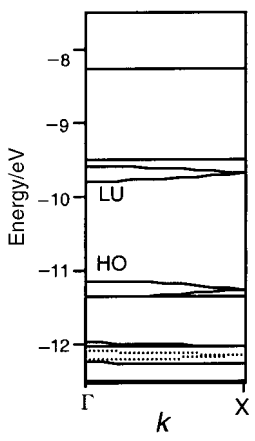

Fig. 10 Band structure of the 1D *meso*-to-*meso* directly linked porphyrin polymer 1D(Q).

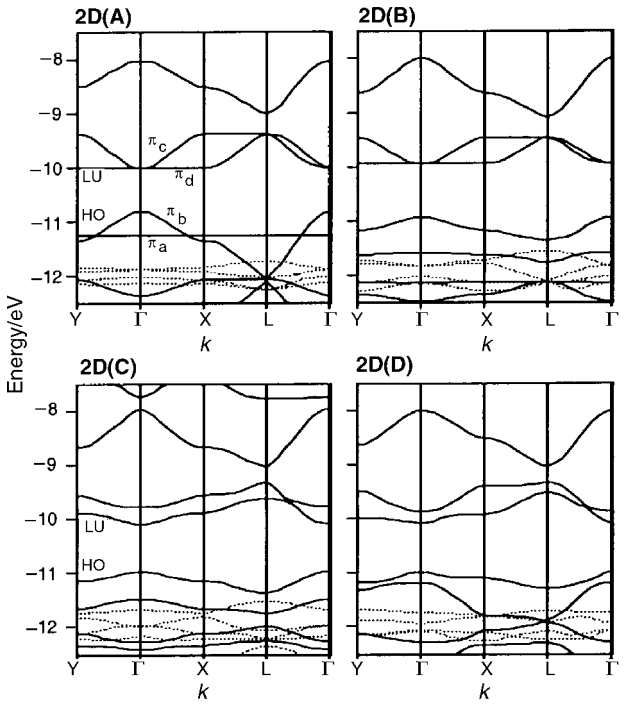

Fig. 11 Band structures of the 2D porphyrin polymer sheets [2D(A)–2D(D)]. The labels Γ, X, Y, and L designate the *k*-points of (0,0), (π/a,0), (0,π/b), and (π/a,π/b), respectively, where *a* and *b* are the unit lengths of the *a* and *b* axes.

from 1D to 2D in the *meso*-to-*meso* porphyrin polymer resulted in an increase of the HO bandwidth (1.26 eV) and decrease of the bandgap (0.79 eV), as presented in Table 3. It is interesting that the electron affinity (10.01 eV) and LU bandwidth (0.63 eV) of 2D(A) are not perturbed at all from those of 1D(A).

Bridging between the β-positions forms two different types of polymers, 2D(B) and 2D(C). 2D(B) has a unit cell of C_{4h} symmetry and similar band structure to that of 2D(A) where the HO and LU bandwidths of 2D(B) (0.42 and 0.48 eV, respectively) are smaller and the bandgap (0.98 eV) is larger. The unit cell of 2D(C) has two-fold symmetry (D_{2h}), causing removal of the degeneracy of the LUCO and (LU+1)CO at the Γ point. Compared with 2D(B), the bandgap becomes smaller (0.88 eV), while the HO and LU bandwidths (0.38 and 0.47 eV, respectively) remain similar. The electron affinity and LU bandwidth of 2D(B) are not perturbed in comparison to those of the corresponding 1D β-to-β porphyrin polymer 1D(E), similar to the case of the 1D and 2D *meso*-to-*meso* porphyrin polymers [1D(A) and 2D(A)] described above. These results imply that the LU- and (LU+1)COs derived from the degenerate e_g MOs of the porphyrin extend along only one of the translational axes in the 2D *meso*-to-*meso* and β-to-β porphyrin polymers.

In the *meso*-to-β porphyrin polymer, 2D(D), the porphyrin rings are connected at the 5,15-*meso*- and 2,12-β-positions along the *a* and *b* axes, respectively. The band structures of 2D(D) along the Γ–X and Γ–Y lines do not reflect those of the

Table 3 The calculated electronic properties (eV) of the 2D porphyrin polymer sheets

	Ionization potential	Electron affinity	HO bandwidth	LU bandwidth	Bandgap
2D(A)	10.80	10.01	1.26	0.63	0.79
2D(B)	10.93	9.95	0.42	0.48	0.98
2D(C)	10.98	10.10	0.38	0.47	0.88
2D(D)	10.99	10.10	0.32	0.58	0.89

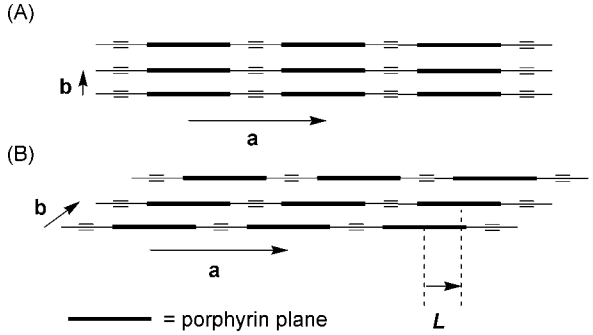

Fig. 12 Schematic illustration of the stacked arrays of 1D *meso*-to-*meso* linear porphyrin polymers 1D(A) with the translational axes and the lateral sliding value *L*: (A) the straight stacked structure ($L=0$), (B) laterally slid structure.

5,15-*meso*-to-*meso* and 2,12-β-to-β 1D porphyrin polymers [1D(A) and 1D(E)], respectively, due to the lower symmetry of the unit cell of 2D(D). There is no crossing between the HO and the (HO−1) bands and between the LU and the (LU+1) bands like in 2D(C). The electronic properties of 2D(D) almost resemble those of 2D(C) except for the LU bandwidth.

All the 2D ethynyl-bridged porphyrin polymer sheets studied here exhibit increased π-conjugation as a whole compared with the corresponding 1D polymers. It is natural that dimensionality and the number of bridging units in a conjugated polymeric system should be crucial in controlling the π-conjugation.

Stacked 1D porphyrin polymers

An infinitely stacked array of 1D linear porphyrin polymers, as illustrated in Fig. 12, is another type of 2D sheet and is also of interest in that its electronic properties can be further modified by an interchain interaction. It is well known that porphyrin oligomers tend to stack and form aggregates[10a] as well as rigid-rod linear polymers.[2b,36] Such stacking patterns should depend on the steric and electronic properties of the peripheral substituents and on the electronic properties of the porphyrin π-system. It has already been discussed whether charge mobilities in self-organized conjugated polymers are affected by the interchain π–π stacking interaction.[4,37]

In order to reveal the structural effect of supramolecular stacked systems on the electronic properties, the band structures of ideally stacked systems of the 1D *meso*-to-*meso* ethynyl-bridged linear porphyrin polymers 1D(A) are also

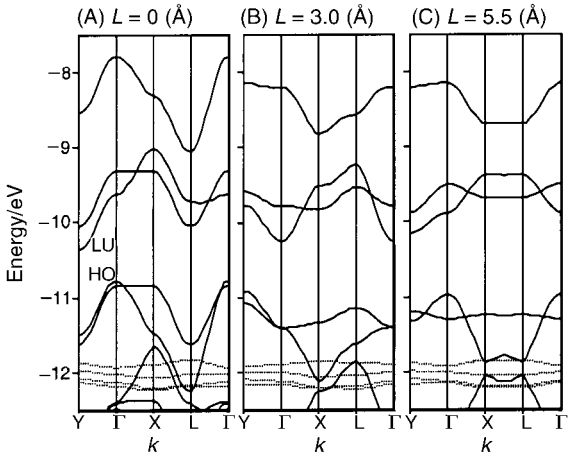

Fig. 13 Band structures of the stacked arrays of 1D *meso*-to-*meso* linear porphyrin polymers 1D(A) with different *L* values: (A) $L=0$ Å, (B) $L=3.0$ Å and (C) $L=5.5$ Å. The labels Γ, X, Y, and L designate the same *k*-points as in Fig. 11.

Table 4 The calculated electronic properties (eV) of the infinitely stacked arrays of 1D porphyrin polymers for different L values

Lateral-sliding value (L)/Å	Ionization potential	Electron affinity	HO bandwidth	LU bandwidth	Direct bandgap	Indirect bandgap
0.0	10.78	10.37	1.47	1.36	1.14	0.41
3.0	10.92	10.25	1.20	1.02	1.15	0.67
5.5[a]	10.97	10.15	0.91	0.77	1.04	0.82

[a]Center of the ethynyl bridge is right above the Zn atom in the adjacent polymer chain at this L value.

investigated here. In the calculation of the stacked polymers in Fig. 12, the interplanar distance is set at 3.5 Å.[38,39]

First, the band structure of the straight stacked polymers (see Fig. 12(A)) is shown in Fig. 13(A). Note that the Γ–X and Γ–Y lines reflect the intrachain and interchain interactions, respectively. Along the Γ–X line, the energy levels of the frontier π bands are destabilized compared with the single linear porphyrin polymer 1D(A) due to an antibonding interaction at the Γ point between the porphyrin rings along the stacking directions. Both the HO and LU bandwidths, however, are significantly enhanced (1.47 and 1.36 eV, respectively) from those of 1D(A), with the direct bandgap being practically intact as listed in Table 4. Such large HO and LU bandwidths indicate that electronic delocalization is well achieved in the straight stacked polymers. Concomitant with the large bandwidths along the Γ–Y line, the stacked systems would show increased carrier mobility along the stacking direction. Moreover, the rather large electron affinities suggest the possibility of n-type doping. A change of morphology by lateral sliding (L) of the linear polymer chains along the a axis (see Fig. 12(B)) would be of further interest. It is found that the band structures do not necessarily change with L in a continuous manner (see Fig. 13 and ESI, Fig. I). These results are surprising in that the interchain interaction is strong and specific, in spite of the rather large interchain distance of 3.5 Å in the range of weak van der Waals interactions for conventional organic substances; even considering the extended Hückel framework suppresses the effect of the interelectron exchange repulsion interaction.

In the stacked porphyrin polymers, the actual bandgaps are all indirect (Table 4) and thus would contribute little to the optical transitions. The direct bandgaps of the stacked polymers remain almost the same value as in the single polymer 1D(A), independent of the lateral sliding value L. This indicates that the lowest optical transition energies of the stacked polymers are kept nearly constant by the π–π stacked structures. It has been reported that neither the cast film of butadiynyl porphyrin polymer nor the dimer aggregate in CH_2Cl_2 shows red-shifts of the lowest absorption band from those of the single ones,[10a,40] the behavior of which resembles the model systems discussed here. Note, however, that the 2D porphyrin polymer sheets examined in the previous section have a direct bandgap for the optical transitions.

Conclusion

1D and 2D ethynyl-bridged porphyrin polymers with various linkage modes were examined by the use of the TBCO method based on the extended Hückel approximation. There are four major findings in the present study.

(i) The *meso*-to-*meso* linear porphyrin polymer is an ideal system with which to maximize π-conjugation through the ethynyl bridges. The β-to-β linear polymer also shows efficient π-conjugation, although the HO and LU bandwidths are reduced from those of the *meso*-to-*meso* polymer. The coplanar structure between the porphyrin rings along the polymer chain is one of the most important factors in maximizing π-conjugation.

(ii) Porphyrin is more efficient in extending π-conjugation through ethynyl bridges than phthalocyanine, although phthalocyanine itself has a more extended π-system. The electronic structures of the porphyrin polymers that we have studied here aid in the design of conjugated porphyrinic materials in which π-conjugation along the polymer chain is finely tuned.

(iii) The band structures of the 2D porphyrin polymer sheets show larger bandwidths and smaller bandgaps than those of the corresponding 1D porphyrin polymers.

(iv) The stacked arrays of porphyrin polymers show even larger bandwidths and smaller indirect bandgaps, while the direct bandgaps remain almost the same as those of the corresponding 1D porphyrin polymer.

Thus, 2D porphyrin polymer sheets could be used as different supramolecular systems to control the charge mobilities and optical transitions of optoelectronic materials. In addition, the present study is also applicable to the molecular design and syntheses of oligomeric and even dimeric ethynyl porphyrins. The combination of the present calculations and sophisticated synthetic methods[9,10,32,41–44] of the conjugated porphyrin polymers will open up a new stage of electronic materials with well-ordered structures, helping the prediction and fine tuning of their electronic properties.

Acknowledgements

Numerical calculations were carried out at the Data Processing Center of Kyoto University.

References

1 T. A. Skotheim, R. L. Elsenbaumer and J. R. Reynolds, *Handbook of Conducting Polymers*, 2nd edn., Marcel Dekker, New York, 1997.
2 (*a*) J. L. Brédas, C. Adant, P. Tackx, A. Persoons and B. M. Pierce, *Chem. Rev.*, 1994, **94**, 243; (*b*) C. Weder, M. S. Wrighton, R. Spreiter, C. Bosshard and P. Günter, *J. Phys. Chem.*, 1996, **100**, 18931.
3 R. H. Friend, R. W. Gymer, A. B. Holmes, J. H. Burroughes, R. N. Marks, C. Taliani, D. D. C. Bradley, D. A. Dos Santos, J. L. Brédas, M. Lögdlund and W. R. Salaneck, *Nature*, 1999, **397**, 121.
4 H. Sirringhaus, P. J. Brown, R. H. Friend, M. M. Nielsen, K. Bechgaard, B. M. W. Langeveld-Voss, A. J. H. Spiering, R. A. J. Janssen, E. W. Meijer, P. Herwig and D. M. de Leeuw, *Nature*, 1999, **401**, 685.
5 (*a*) G. Yu, J. Gao, J. C. Hummelen, F. Wudl and A. J. Heeger, *Science*, 1995, **270**, 1789; (*b*) M. Granström, K. Petritsch, A. C. Arias, A. Lux, M. R. Andersson and R. H. Friend, *Nature*, 1998, **395**, 257.
6 For reviews, see: (*a*) M. R. Wasielewski, *Chem. Rev.*, 1992, **92**, 435; (*b*) M. G. H. Vicente, L. Jaquinod and K. M. Smith, *Chem. Commun.*, 1999, 1771; (*c*) P. F. H. Schwab, M. D. Levin and J. Michl, *Chem. Rev.*, 1999, **99**, 1863.
7 J. P. Collman, J. E. Hutchison, M. A. Lopez, A. Tabard, R. Guilard, W. K. Seok, J. A. Ibers and M. L'Her, *J. Am. Chem. Soc.*, 1992, **114**, 9869.
8 H. L. Anderson, *Chem. Commun.*, 1999, 2323.
9 (*a*) V. S.-Y. Lin, S. G. DiMagno and M. J. Therien, *Science*, 1994, **264**, 1105; (*b*) V. S.-Y. Lin and M. J. Therien, *Chem. Eur. J.*, 1995, **1**, 645.
10 (*a*) H. L. Anderson, *Inorg. Chem.*, 1994, **33**, 972; (*b*) P. N. Taylor, J. Huuskonen, G. Rumbles, R. T. Aplin, E. Williams and H. L. Anderson, *Chem. Commun.*, 1998, 909; (*c*) P. N. Taylor, A. P. Wylie, J. Huuskonen and H. L. Anderson, *Angew. Chem., Int. Ed.*, 1998, **37**, 986; (*d*) P. N. Taylor and H. L. Anderson, *J. Am. Chem. Soc.*, 1999, **121**, 11538.
11 D. P. Arnold and D. A. James, *J. Org. Chem.*, 1997, **62**, 3460.

12 B. Jiang, S.-W. Yang, D. C. Barbini and W. E. Jones Jr., *Chem. Commun.*, 1998, 213.
13 D. P. Arnold and G. A. Heath, *J. Am. Chem. Soc.*, 1993, **115**, 12197.
14 K. Tanaka, N. Kosai, H. Maruyama and H. Kobayashi, *Synth. Met.*, 1998, **92**, 253.
15 R. Hoffmann, C. Janiak and C. Kollmar, *Macromolecules*, 1991, **24**, 3725.
16 R. Hoffmann, *J. Chem. Phys.*, 1963, **39**, 1397.
17 A. M. Schaffer, M. Gouterman and E. R. Davidson, *Theor. Chim. Acta*, 1973, **30**, 9.
18 A. Vela and J. L. Gázquez, *J. Phys. Chem.*, 1988, **92**, 5688.
19 J. H. Ammeter, H.-B. Bürgi, J. C. Thibeault and R. Hoffmann, *J. Am. Chem. Soc.*, 1978, **100**, 3686.
20 (*a*) S. Y. Hong and D. S. Marynick, *J. Chem. Phys.*, 1992, **96**, 5497; (*b*) S. Y. Hong and J. M. Song, *J. Chem. Phys.*, 1997, **107**, 10607.
21 M.-H. Whangbo and K. R. Stewart, *Isr. J. Chem.*, 1983, **23**, 133.
22 E. Canadell and S. Alvarez, *Inorg. Chem.*, 1984, **23**, 573.
23 P. Gomez-Romero, Y.-S. Lee and M. Kertesz, *Inorg. Chem.*, 1988, **27**, 3672.
24 G. Frapper and M. Kertesz, *Inorg. Chem.*, 1993, **32**, 732.
25 N. Re, A. Sgamellotti and C. Floriani, *J. Chem. Soc., Dalton Trans.*, 1998, 2521.
26 (*a*) K. Tanaka, T. Saito, Y. Oshima, T. Yamabe and H. Kobayashi, *Chem. Phys. Lett.*, 1997, **272**, 189; (*b*) T. Saito, Y. Akita, H. Kobayashi and K. Tanaka, *Synth. Met.*, 2000, **108**, 67.
27 M. Gouterman, *J. Mol. Spectrosc.*, 1961, **6**, 138.
28 (*a*) E. M. Maya, P. Vázquez and T. Torres, *Chem. Commun.*, 1997, 1175; (*b*) E. M. Maya, P. Vázquez and T. Torres, *Chem. Eur. J.*, 1999, **5**, 2004.
29 R. Stranger, J. E. McGrady, D. P. Arnold, I. Lane and G. A. Heath, *Inorg. Chem.*, 1996, **35**, 7791.
30 R. Kumble, S. Palese, V. S.-Y. Lin, M. J. Therien and R. M. Hochstrasser, *J. Am. Chem. Soc.*, 1998, **120**, 11489.
31 The rotational-angle dependent band structures are calculated in an alternately tilted structure, *i.e.*, all the odd numbered and all the even numbered rings are, respectively, located on two planes, the tilting angle between which is defined as the rotational angle.
32 G. S. Wilson and H. L. Anderson, *Chem. Commun.*, 1999, 1539.
33 (*a*) K. Susumu, T. Shimidzu, K. Tanaka and H. Segawa, *Tetrahedron Lett.*, 1996, **37**, 8399; (*b*) A. Osuka and H. Shimidzu, *Angew. Chem., Int. Ed. Engl.*, 1997, **36**, 135; (*c*) N. Aratani, A. Osuka, Y. H. Kim, D. H. Jeong and D. Kim, *Angew. Chem., Int. Ed.*, 2000, **39**, 1458.
34 A. J. Berresheim, M. Müller and K. Müllen, *Chem. Rev.*, 1999, **99**, 1747.
35 (*a*) R. H. Baughman, H. Eckhardt and M. Kertesz, *J. Chem. Phys.*, 1987, **87**, 6687; (*b*) F. Diederich and Y. Rubin, *Angew. Chem., Int. Ed. Engl.*, 1992, **31**, 1101; (*c*) J. K. Burdett and A. K. Mortara, *Chem. Mater.*, 1997, **9**, 812; (*d*) U. H. F. Bunz, Y. Rubin and Y. Tobe, *Chem. Soc. Rev.*, 1999, **28**, 107.
36 C. E. Halkyard, M. E. Rampey, L. Kloppenburg, S. L. Studer-Martinez and U. H. F. Bunz, *Macromolecules*, 1998, **31**, 8655.
37 R. Österbacka, C. P. An, X. M. Jiang and Z. V. Vardeny, *Science*, 2000, **287**, 839.
38 C. A. Hunter and J. K. M. Sanders, *J. Am. Chem. Soc.*, 1990, **112**, 5525.
39 Note that the HO and the LU bandwidths significantly change with the interplanar distance of 1D porphyrin polymers.
40 K. Pichler, H. L. Anderson, D. D. C. Bradley, R. H. Friend, P. J. Hamer, M. G. Harrison, C. P. Jarrett, S. J. Martin and J. A. Stephens, *Mol. Cryst. Liq. Cryst.*, 1994, **256**, 415.
41 R. W. Wagner, J. Seth, S. I. Yang, D. Kim, D. F. Bocian, D. Holten and J. S. Lindsey, *J. Org. Chem.*, 1998, **63**, 5042.
42 K. Sugiura, Y. Fujimoto and Y. Sakata, *Chem. Commun.*, 2000, 1105.
43 H. Segawa, F.-P. Wu, N. Nakayama, H. Maruyama, S. Sagisaka, N. Higuchi, M. Fujitsuka and T. Shimidzu, *Synth. Met.*, 1995, **71**, 2151.
44 T. Ogawa, Y. Nishimoto, N. Yoshida, N. Ono and A. Osuka, *Chem. Commun.*, 1998, 337.